Chapter 20

Reverse Osmosis

20.1 INTRODUCTION

The seawater or brackish water desalination process by reverse osmosis (RO) has been known for many years. Loeb and Sourirajan (1962) developed a method for making asymmetric cellulose acetate membranes, which provide excellent scope for the application of this process for practical purposes due to their relatively high water fluxes and separation efficiency (Williams, 2003). Among the synthetic polymeric membranes on the market is the aromatic polyamide with pendant sulfonic acid group proposed by DuPont (Uemura and Henmi, 2008). It has a high rejection performance, which can be used for single-stage seawater or brackish water desalination. The development of new-generation membranes such as thin-film, composite (with an in situ monomer condensation method), nanostructure, and mixed matrix membranes that can have much higher water flux and solute separation properties has resulted in many additional RO applications such as wastewater treatment, e.g., in the galvanic industry, for water softening, and for food and beverage processing (Bhattacharyya and Williams, 1992). Nowadays, there are growing activities in developing RO membranes from inorganic materials such as ceramic membranes (e.g., α-alumina supported MFI-type zeolite membranes) due to their thermal, mechanical, and chemical properties. Zeolite membranes could be an alternative for polymeric membranes in treating various kinds of water and wastewater, and/or for the separation of organic mixtures (Lee et al., 2011).

One of the most important applications of RO is water treatment for producing high-quality water using high-salinity geothermal water, surface water, peat water (natural brown water), as well as wastewater (industrial, municipal water) treatment. RO is capable of removing low concentration bioactive pollutants such as pesticides and hormones from surface water (Hofman et al., 1997). Potential application of the RO process is the concentration of various fruit juices (orange, apple, pear, grape, tomato juices) and preconcentration of sugar juices. This process is also widely applied in the dairy industry for, e.g., recovering protein, defatting whey, and concentrating milk and whey as alternatives to conventional processes (Pouliot, 2008). Other applications of the RO process are, e.g., alcohol removal from fermented beverages and separation of organic mixtures, including alcohols and hydrocarbon (azeotropic, isomeric) mixtures (Koops et al., 2001).

Fouling/biofouling is regarded as the most serious problem in the RO process, depending on the water composition used for separation. Reasons for fouling of the RO membrane are chemical (adsorption of organic materials) and biological fouling (microbe adsorption by hydrophobic or electrostatic interaction, deposition of exhaust material of biological metabolism) (Uemura and Henmi, 2008). This is why it is important to produce a low-fouling property membrane with high water flux and stable operation.

The osmotic pressure π of the solution can be calculated by van't Hoff's equation:

$$\pi = \nu_i R T C_i \tag{20.1}$$

where π is the osmotic pressure, Pa; R is the gas constant (R=8.3145 m³Pa/(K mol), T is the absolute temperature (K), ν_i is the number of different dissociated ions (e.g. this number is equal to 2 in case of NaCl) and C_i is the concentration of component i (mol/m³). The concentration should be multiplied by two for, e.g., NaCl solute because it dissociates into two ions. When the osmotic pressure is predicted for high concentration of solutions, a virial expansion expression can be used:

$$\pi = \nu_i R T C_i + B C_i^2 + E C_i^3 + \cdots \tag{20.2}$$

where B and E are constants. Macromolecular solutions often use:

$$\pi = A C_i^n \quad \text{with } n > 1. \tag{20.3}$$

The osmotic pressure of NaCl as a function of concentration and the hydraulic pressure regime needed for RO, etc. are shown in Chapter 21.

20.2 MEMBRANE TRANSPORT MODELS

For a dense membrane the most popular transport model is the "solution/diffusion" model, in which penetrants dissolve at the membrane interface and then diffuse through the membrane along the concentration gradient. Separation occurs due to the differences in solubility and diffusivity of permeates. Lonsdale et al. (1965) proposed the solution/diffusion model to describe transport in "nonporous" membranes. Transport is a result of concentration (activity) and pressure gradients across the membrane. The chemical potential difference ($\Delta\mu$) is given by (see Section 3.3.1 for more details):

$$\Delta\mu_i = RT \ln \Delta a_i + V_i \Delta P \tag{20.4}$$

where a_i is the activity of the solute or solvent, V_i is the molar volume (m³/mol), ΔP is the pressure differential across the membrane (Pa), and μ is the chemical potential (J/mol). The variation of P, μ, and a are shown in Fig. 20.1. Pressure in the membrane is uniform and equal to the high-pressure value; the chemical potential gradient within the membrane is expressed as a concentration gradient. The water flux is derived from Henry's law and Fick's first law of diffusion in the presence of hydraulic pressure difference, ΔP, and is related to water permeability as follows (Wijmans and Baker (1995, 2006) (Wang et al., 2014):

$$J_w = \frac{DHC_w^o}{\delta}\left(1 - \exp\left[\frac{-V_i(\Delta P - \Delta\pi)}{RT}\right]\right) \tag{20.5}$$

The exponent of the exponential term in Eq. (20.5) tends to zero under practical conditions for water, thus its simplification gives (Wijmans and Baker, 1995, 2006; Wang et al., 2014):

$$J_w = A(\Delta P - \Delta\pi) = \frac{HD_wC_w^o}{\delta}\frac{V_w}{RT}(\Delta P - \Delta\pi) \tag{20.5a}$$

with:

$$A = \frac{H_wD_w}{\delta}\frac{V_w}{RT} \tag{20.5b}$$

where D_w is the water diffusion coefficient (m²/s), A is the water permeability (m/s bar), H_w is the water membrane partition coefficient (kg/m³membrane/kg/m³solution), R is the universal gas constant (J/molK), T is the absolute temperature (K), δ is the membrane thickness (m), V_w is the molar volume of water (m³/mol), and C_w^o is the mole concentration of water in the feed phase (mol/m³). Similarly, the solute flux can be obtained by methodology used in Section 18.3 (see the paper of Wijmans and Baker, 2006). Thus the solute transfer rate is derived from Fick's law with the assumption that the driving force is almost entirely due to concentration differences:

$$J_s = B(C_m - C_p) = \frac{D}{\delta}(\phi^* - \phi_\delta^*) \equiv \frac{DH}{\delta}(C_m - C_p) \tag{20.6}$$

with:

$$HC_m = \phi^*; \quad HC_p = \phi_\delta^*; \quad B = k^oH; \quad k^o = \frac{D}{\delta}$$
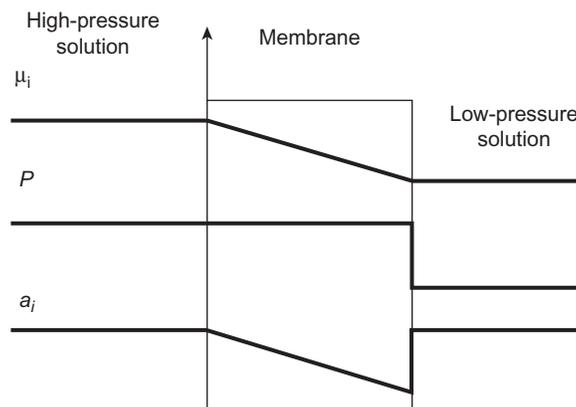
FIGURE 20.1   Chemical potential, μ_i, pressure, P, and solvent activity, a_i, in a reverse osmosis membrane according to the solution/diffusion model (Wijmans and Baker, 1995).

where B is the solute permeability (m/s), D is the diffusion coefficient through the active membrane layer (m²/s), H is the solute solubility in the nonporous membrane, δ is the thickness of the active layer (m), ϕ^* is the feed-side membrane interface concentration (kg/m³), and ϕ_δ^* is the concentration at the outlet membrane surface (kg/m³) (see Fig. 20.2 for nomenclature for the fluid phases). The question is often asked whether this equation is always applicable to dense membranes. All producers want to prepare active membrane layer with larger and larger water permeability. What kind of change in its structure can occur at high water flux? Soltanieh and Gill (1981) stated that the pore flow can also be important at high water flux. Jaroshchuk (2004, 2012) recommended a solution/diffusion imperfection model for high water flux. Important parameters of the membrane separation processes are the observed and real rejection coefficients, respectively:

$$R_o = 1 - \frac{C_p}{C_b} \tag{20.7}$$

and:

$$R_r = 1 - \frac{C_p}{C_m}. \tag{20.8}$$

20.2.1 Irreversible Thermodynamics Model

Membrane transport models based on the principle of irreversible thermodynamics approach transport with hydraulic and osmotic pressure gradients and fluxes obtained from phenomenological thermodynamic relationships (Geens et al., 2006). The Kedem−Katchalsky model (1963) defines J_w as a function of transmembrane pressure gradient as (J_w is the solvent volumetric transport rate, m³/m²):

$$J_w = A(\Delta P - \sigma \Delta \pi). \tag{20.9}$$

The reflection coefficient, σ, was introduced to characterize flux interactions when water and solute cross the dense membrane. If $\sigma < 1$ indicates a semipermeable membrane, then $\sigma = 1$ indicates an impermeable membrane (complete rejection) (Wijmans and Baker, 1995). In the case of binary solutions, the transport of solutes can be given as:

$$J_s = B\Delta \pi + (1 - \sigma)\phi_{avg} J_w \tag{20.10}$$

where ϕ_{avg} is the average concentration in the membrane pores. The real rejection can be expressed as (Wang et al., 2014):

$$R_r = \frac{\phi_{avg} J_w + \omega \Delta \pi}{\sigma \phi_{avg} J_w}. \tag{20.11}$$

The Kedem−Katchalsky model was modified by Spiegler and Kedem to avoid the concentration dependency of the model coefficients (Spiegler and Kedem, 1966). The Spiegler−Kedem model characterizes membranes in two
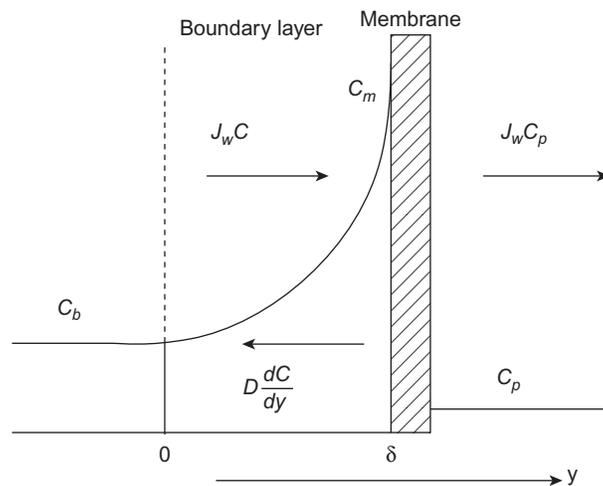
FIGURE 20.2 Concentration distribution and nomination in the polarization layer of the reverse osmosis membrane.

parameters: solute permeability, B, and reflection coefficient, σ, and these parameters have no dependence on concentration. The value of J_w is the same as that in the Kedem−Katchalsky model, while the solute flux is defined as:

$$J_s = B\delta\frac{d\phi}{dy} + (1 - \sigma)J_w\phi. \tag{20.12}$$

Integration of Eq. (20.12) over the membrane yields the rejection coefficient (Peng et al., 2010):

$$R_r = 1 - \frac{C_p}{C_m} = \sigma\left(\frac{1 - Y}{1 - \sigma Y}\right) \tag{20.13}$$

with:

$$Y = \exp\left(\frac{J_w(1 - \sigma)}{B}\right). \tag{20.14}$$

The Siegler−Kedem model is usually coupled with liquid film theory to yield (Peng et al., 2010):

$$\frac{R_o}{1 - R_o} = \frac{\sigma}{1 - \sigma}\left\{1 - \exp\left[-\frac{J_w(1 - \sigma)}{B}\right]\right\}\exp\left(-\frac{J_w}{k_d}\right) \tag{20.15}$$

where R_o is the observed rejection coefficient and k_d is the draw phase liquid mass transfer coefficient (m/s).

20.2.2 External Concentration Polarization

During pressure-driven membrane filtration, the convective solvent flux transports solutes toward the membrane, which leads to a concentration increase in the boundary layer at the membrane surface. According to Fig. 20.2, concentration polarization can be described at steady state by the following equality:

$$J_w C - D\frac{dC}{dy} = J_w C_p \tag{20.16}$$

where J_w is the water flux through the boundary layer perpendicular to the membrane surface (m/s), C is the concentration at a given y value (kg/m^3), D is the solute diffusion coefficient (m^2/s), C_p is the product concentration (kg/m^3), and y is the local coordinate (m). Accuracy of this equation can easily be stated by means of Fig. 20.1. The boundary conditions are also given in the figure, namely:

$$y = 0 \quad \text{then} \quad C = C_b \tag{20.17a}$$

$$y = \delta_L \quad \text{then} \quad C = C_m. \tag{20.17b}$$

Eq. (20.16) is solved by integration over the boundary conditions as:

$$\frac{C_m - C_p}{C_b - C_p} = e^{Pe_L} \tag{20.18}$$

with:

$$Pe_L = \frac{J_w\delta_L}{D_L} = \frac{J_w}{k_L} \tag{20.19}$$

where k_L is the diffusive mass transfer coefficient in the fluid boundary layer (m/s) and subscript L marks the boundary layer. After differentiating Eq. (20.16) the concentration distribution can also be determined (Nagy, 2014). Thus one can obtain:

$$J_w\frac{dC}{dy} - D\frac{d^2C}{dy^2} = 0. \tag{20.20}$$

Its general solution is ($Y = y/\delta_L$):

$$C = Te^{Pe_L Y} + S. \tag{20.21}$$

Applying the boundary conditions given by Eqs. (20.17a) and (20.17b), the concentration distribution is (for details see Section 7.2.1):

$$C = \frac{C_b - C_m}{1 - e^{Pe_L}}e^{Pe_L Y} + \frac{C_m - C_b e^{Pe_L}}{1 - e^{Pe_L}}. \tag{20.22}$$

Thus the solute transfer rate will be:

$$J_s = \beta_L(C_b e^{Pe_L} - C_m) \tag{20.23}$$

with:

$$\beta_L = \frac{k_L Pe_L}{e^{Pe_L} - 1}. \tag{20.23a}$$

Putting $J = J_w C_p$ into Eq. (20.23), one gets Eq. (20.18). Applying Eq. (20.23) for all mass transfer layers, in which diffusive and convective mass transport take places simultaneously, or only diffusive transport (as is the case in the active membrane layer), the resistance-in-series model can easily be applied to the description of the mass transport process. This transport process is deeply analyzed in Chapter 7 with different configurations of the mass transport layers and different transport directions. In Chapter 7, the dense membrane layer is not considered anymore as a "black box," but diffusive transport across the active layer is combined with convective transport through the polarization layer. Thus new transport expressions were obtained using Eq. (20.23) as it is discussed in the following sections (Fig. 20.3).

20.2.3 Overall Mass Transfer Rate (Polarization Plus Membrane Layers)

The mass transfer rates to be considered for expressing the overall mass transfer rate are shown in Eq. (20.6), given for the active membrane layer, and in Eq. (20.23), given for the polarization layer, namely:

$$J_s = k^o\left(\phi^* - \phi_\delta^*\right) \tag{20.6a}$$

and:

$$J_s = \beta_L(C_b e^{Pe_L} - C_m) \tag{20.23}$$

with:

$$k^o = \frac{D}{\delta}; \quad \beta_L = \frac{k_L Pe_L}{e^{Pe_L} - 1}$$
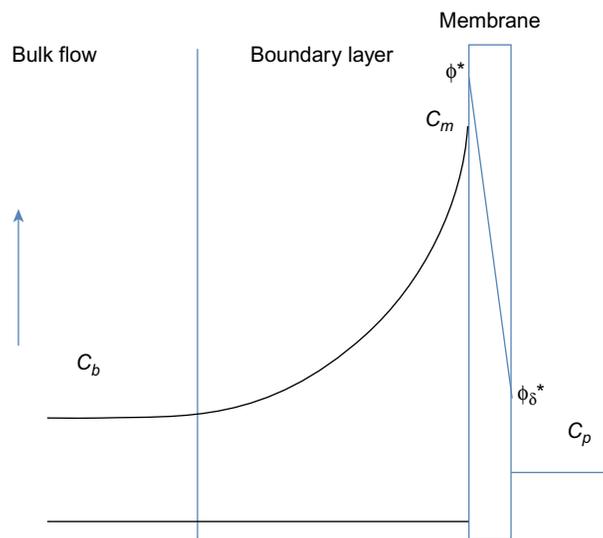
FIGURE 20.3 Solute concentration distribution in the polarization and membrane layers and the nomination. According to the concentration distribution in the membrane layer it is clear that the transport takes place by the solution/diffusion mechanism across it (Eq. 20.6a), while for the polarization layer the transfer rate is defined by Eq. (20.23).

where k^o is the diffusive mass transfer coefficient of the active membrane layer (m/s), H is the solubility coefficient ($HC_m = \phi^* HC_p = \phi^*_\delta$), and δ is the thickness of the active membrane layer (m). Equating Eqs. (20.6a) and (20.23), the overall mass transfer rate then is:

$$J_{s,ov} = \beta_{ov}(C_b e^{Pe_L} - C_p) \tag{20.24}$$

with:

$$\frac{1}{\beta_{ov}} = \frac{1}{\beta_L} + \frac{1}{k^o H}. \tag{20.25}$$

Taking into account that $J = J_w C_p$, product concentration can be expressed as:

$$C_p = \frac{\beta_{ov} C_b e^{Pe_L}}{J_w + \beta_{ov}}. \tag{20.26}$$

Enhancement can then be obtained by putting Eq. (20.25) into Eq. (20.26), thus:

$$E = \frac{C_p}{C_b} = \frac{1}{1 + J_w e^{-Pe_L}/(k^o H)}. \tag{20.27}$$

Intrinsic enhancement can also be expressed, starting from the following equation:

$$\beta_{ov}(C_b e^{Pe_L} - C_p) = J_w C_p. \tag{20.28}$$

Putting Eq. (20.27) into the reformed Eq. (20.28), intrinsic enhancement can be obtained as:

$$E_o = \frac{C_p}{C_m} = 1 \Big/ \left\{ \frac{e^{Pe_L}}{E} - \frac{J_w}{\beta_{ov}} \right\}. \tag{20.29}$$

Combining the mass transfer rate through the membrane active layer with that given by the polarization layer, new expressions can be expressed for the interface concentrations, namely C_m and C_p as a function of the mass transport parameters k_L, J_w, and k^o.

Integration of the cake layer formed on the active layer can easily be made (not shown here) as done, e.g., in Chapter 10.

20.2.4 Mass Transfer Rate in the Presence of the Fouling (or Cake) Layer

The fouling layer increases the transport layers in the pathway of the solute component, namely the polarization layer and the active membrane layer are completed by the cake layer. This situation is plotted in Fig. 10.4 where both the cake (and polarization) layers are forming on the feed side of membrane. As we know there is no concentration gradient in the membrane support layer, because there is no sweeping phase on the permeate side. The solution methodology will be the same as discussed in Section 10.2.4. The only deviation in the mass transfer rates of the layers is that diffusive mass transport takes place in the membrane active layer only. Thus the transfer rates of the transport layers are:

$$J_i^o = \beta_L^o(C_i^o - e^{-Pe_L} C_{c,i}) \tag{20.30}$$

$$J_i^o = \beta_c^o(C_{c,i} - e^{-Pe_c} C_{m,i}) \tag{20.31}$$

$$J_i^o = k^o(HC_{m,i} - HC_{p,i}) \tag{20.32}$$

with:

$$\beta_L^o = \frac{J_w}{e^{-Pe_L} - 1}; \quad \beta_c^o = \frac{J_w}{e^{-Pe_c} - 1}; \quad k^o = \frac{D}{\delta}$$

where subscripts L, c, m denote the polarization layer, the cake layer, and the membrane active layer, respectively ($HC_{m,i} = \phi_i^*$; $HC_{p,i} = \phi_{\delta,i}^*$) and D and δ are the diffusion coefficient in the active membrane layer and the membrane active layer's thickness, respectively. The overall mass transfer rate is:

$$J_{ov,i}^o = \beta_{ov}^o(C_i^o - e^{-(Pe_L + Pe_c)} C_{p,i}) \tag{20.33}$$

with:

$$\frac{1}{\beta_{ov}^o} = \frac{1}{\beta_L^o} + \frac{e^{-Pe_L}}{\beta_c^o} + \frac{e^{-(Pe_L + Pe_c)}}{H_i k^o}.$$ (20.34)

On the other hand, the value of the permeate rate can be expressed by the water flux and permeate concentration, thus:

$$J_i^o = J_w C_{p,i}.$$ (20.35)

Eqs. (20.33) and (20.34) are equal to each other. Thus equating these two expressions, the value of the outlet concentration can be expressed as:

$$C_{p,i} = \frac{\beta_{ov}^o}{J_w + \beta_{ov}^o e^{-(Pe_L + Pe_c)}} C_i^o.$$ (20.36)

The concentration distribution can be given for every single transport layer. In the knowledge of concentration distributions' equation, still the interface concentration should be dtermined as it was done e.g., in Section 10.2.4 by Eqs. (10.50) and (10.52).

20.3 CONCLUDING REMARKS

RO is a widely applied membrane separation process with known transport expression. This chapter briefly summarized these expressions focusing on the irreversible thermodynamic model. Then, the mass transfer rate given for the membrane active layer was integrated into that given for the polarization layer expressing the overall mass transfer rate. By means of the overall mass transfer rate and the outlet transfer rate, both the enrichment and intrinsic enrichment factors were expressed with the mass transport parameters of the process.

REFERENCES

Bhattacharyya, D., Williams, M., 1992. Theory- Reverse Osmosis in Membrane Handbook. In: Ho, W., Shirkar, K. (Eds.). Van Notstrand Reinhold, New York, pp. 269−280.

Geens, J., Boussu, K., Vandecasteele, C., Van der Bruggen, B., 2006. Modelling solute transport in nonaqueoeus nanofiltration. J. Membr. Sci. 281, 139−148.

Hofman, J.A.M.H., beerendonk, E.F., Folmer, H.C., Kruithof, J.C., 1997. Removal of pesticides and other micropollutants with cellulose-acetetae, polyamide and ultra-low pressure reverse osmosis membranes. Desalination 113, 209−214.

Jaroshchuk, A.E., 2004. The role of imperfection in the solute transfer in nanofiltration. J. Membr. Sci. 239, 9−15.

Jaroshchuk, A.E., 2012. Solution-diffusion-imperfection model revised. J. Membr. Sci. 413, 91−101.

Kedem, O., Katchalsky, A., 1963. Permeability of composite membranes. 1. Electric current, volume flow and flow of solute through membranes. T. Faraday Soc. 59, 1918−1930.

Koops, G.H., Yamada, S., Nakao, S.I., 2001. Separation of linear hydrocarbons and carboxylic acids from ethanol and hexane solution by reverse osmosis. J. Membr. Sci. 189, 241−254.

Lee, K.P., Arnor, T.C., Mattia, D., 2011. A review of reverse osmosis membrane materials for desalination-development to date and future potential. J. Membr. Sci. 370, 1−22.

Loeb, S., Sourirajan, S., 1962. Sea water demineralization by means of an osmotic membrane. Adv. Chem. Ser. 38, 117−132.

Lonsdale, H.K., Merten, U., Riley, R.I., 1965. Transport properties of cellulose acetate osmotic membranes. J. Appl. Polym. Sci. 9, 1341−1362.

Nagy, E., 2014. Resistance-in-series, salt- and water flux models for forward osmosis and pressure retarded osmosis for energy generation. J. Membr. Sci. 460, 71−81.

Peng, F.B., Huang, X.F., Jawor, A., Hoek, E.M.V., 2010. Transport, structural and interfacial properties of poly (vinyl alcohol-polysulfone composite nanofiltration membranes. J. Membr. Sci. 353, 169−176.

Pouliot, Y., 2008. Membrane processes in dairy technology-from a simple idea to world-wide panacea. Int. Dairy J. 18, 735−740.

Soltanieh, M., Gill, W.N., 1981. Review of reverse osmosis membrane and transport models. Chem. Eng. Commun. 12, 279−383.

Spiegler, K.S., Kedem, O., 1966. Thermodynamics of hyperfiltration (reverse osmosis) criteria for efficient membranes. Desalination 1, 1−22.

Uemura, T., Henmi, M., 2008. Thin-film composite membranes for reverse osmosis. In: Li, N.N., Fane, A.G., Ho, W.S.W., Matsuura, T. (Eds.), Advanced Membrane Technology and Applications. Wiley & Sons, New Jersey, pp. 3−20.

Wang, J., Dlamini, D.S., Mishra, A.K., Pendergast, T.M., Wong, M.C.Y., Mamba, B.B., Freger, V., Verliefde, A.R.D., Hoek, E.M.V., 2014. A critical review of transport through osmotic membranes. J. Membr. Sci. 454, 516−537.

Wijmans, J.G., Baker, R.W., 1995. The solution-diffusion model − a review. J. Membr. Sci. 107, 1−21.

Wijmans, J.G., Baker, R.W., 2006. The solution-diffusion model: a unified approach to membrane permeation. In: Yampolskii, Pinnau, Freeman (Eds.), Material Science of Membranes. Wiley and Sons Ltd., England, pp. 160−189.

Williams, M.E., 2003. A Brief Review of Reverse Osmosis Membrane Technology. EET Corporation and Williams Servies Company Inc., pp. 1−24